

First-principles asymptotics for the oscillatory exchange coupling in Co/Cu/Co of (100), (110), and (111) orientations

N. N. Lathiotakis* and B. L. Györfly

H. H. Wills Physics Laboratory, University of Bristol, Royal Fort, Tyndall Avenue, Bristol BS8 1TL, United Kingdom

B. Újfalussy

Research Institute for Solid State Physics, P.O. Box 49, H-1525 Budapest, Hungary

(Received 1 November 1999)

We developed a theory of the oscillatory magnetic coupling across nonmagnetic, ordered or disordered layers and illustrate its use by explicit calculations for Co/Cu/Co trilayers of (100), (110), and (111) orientations. Our approach to the problem is based on the layered, screened Korringa-Kohn-Rostoker (KKR) and KKR-coherent-potential approximation electronic structure methods and employs a saddle-point approximation for calculating the coupling energy for asymptotically large spacer thicknesses D . The results of the asymptotic analysis are tested against full calculations, and other important issues concerning the general validity of the approach are examined. Our results for the oscillation periods as well as the amplitudes and phases are in good agreement with experiments and other calculations.

I. INTRODUCTION

Since the discovery of giant magnetoresistance GMR (Refs. 1,2) and oscillatory exchange coupling³ (OEC) in magnetic multilayers such as Co/Cu/Co sandwiches a decade ago, these phenomena have been among the most popular subjects of both scientific and technological inquiries. The basic experimental geometry in which this phenomenon occurred is depicted in Fig. 1. In short, what is measured is the coupling energy $\delta\Omega_{LR}$ between the magnetization of the layer L , \mathbf{M}_L , and that of layer R , namely \mathbf{M}_R , as a function of the spacer thickness D , and what is found is that the exchange interaction $J(D)$, defined by the relation $\delta\Omega_{LR} = J(D)\mathbf{M}_L \cdot \mathbf{M}_R$ oscillates as a function of D .

It is, by now, well established that the periods of OEC are related to the Fermi surface of the spacer. This is particularly the case for Cu spacers for which this relation has been confirmed quantitatively.^{4,5} In this paper we shall focus on a first-principles theory of the amplitudes and the phases of OEC in the regime of asymptotically large, spacer thickness D .

To summarize the current state of understanding for the particular sandwich structures we shall be concerned with, we recall that epitaxial Co/Cu/Co(100) was the system for which antiferromagnetic (AF) coupling was observed,^{6,7} for five monolayers (ML) of Cu thickness, and subsequently the oscillatory behavior of the interaction was discovered.⁸ Since then the experiments have been repeated many times⁹⁻¹¹ and the emerging picture is that there are two oscillation periods: a short one (≈ 2.5 ML) and a large one ($\approx 5.5-8.0$ ML). The periods predicted from the analysis of the Cu Fermi surface are 2.6 and 5.9 ML for the short and long periods, respectively,^{4,5} in agreement with experiments. At first, both the absolute sizes and the ratios of the amplitudes of the various oscillatory contributions from the first first-principles calculations of the OEC for the (100) orientation¹²⁻¹⁶ failed to agree with experiments. More recently, Lang *et al.*^{12,13}

calculated the OEC for two Co slabs embedded in Cu using Korringa-Kohn-Rostoker (KKR) method and found values for the amplitudes of the right order of magnitude, although to explain the relative sizes of the short and long periods a model of surface roughness had to be invoked.^{12,13}

For the (110) orientation the Fermi surface analysis predicts four different oscillation periods,^{4,16-18} three of which are small and not seen in experiments but the large one is similar in size to the observed oscillation period.^{19,20} The reason for the lack of observing the small periods is still an open question. It is believed, and this work also suggests, that at least one of them should be observed,²¹ since it is found to dominate the coupling in our calculations. The significance of the large oscillation period is that a pronounced feature of the Cu-like Fermi surfaces, namely the neck connecting Fermi surface spheres in the repeated zone scheme, appears to be directly measured by the period of the OEC across Co/Cu/Co(110). Thus, by alloying the Cu spacer with Ni and measuring the oscillation period for this particular growth direction Okuno *et al.*²⁰ measured the change of the neck of $\text{Cu}_{1-x}\text{Ni}_x$ Fermi surface with Ni concentration. Reassuringly they found good agreement with KKR-coherent-potential approximation (CPA) calculations^{17,22} as well as two-dimensional-angular correlation of (positron) annihila-

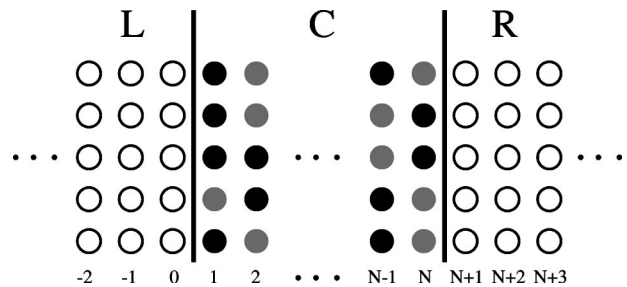


FIG. 1. Schematic view of a sandwich structure of L and R layers separated by a spacer layer C which could be optionally a random binary alloy.

tion radiation (2D-ACAR) measurements.²³

Finally, we turn to trilayers of (111) orientation. From the theoretical point of view these are important examples because only one period is predicted by the Fermi surface analysis^{4,16,17} and hence there is less room for misinterpreting the experiments. Unfortunately, the experimental situation is far from simple. Although OEC had been observed for the sputtered (111) samples,^{24,25} the molecular-beam epitaxy grown ones initially did not show any AF coupling.²⁶ Nevertheless, later, OEC was also observed for the epitaxial samples.²⁷⁻³² In conclusion we note that although (100) has been much studied theoretically there is a lack of such investigation for the (110) and (111) growth directions. This is especially the case for first-principles calculations of interest here. It is one of the aims of the present paper to fill that gap. Namely, we shall provide first-principles calculations for the oscillatory exchange coupling across Cu layers for all the (100), (110), and (111) orientations within the same theoretical framework.

From the theoretical point of view, the attempts to investigate the OEC fall into two main categories: The first is models based on semiphenomenological approaches which usually involve asymptotic analysis for large spacer thickness.^{4,5,33,34} The second is a first-principles approach based on density-functional calculations of the total energy.^{21,35,36} In what follows we shall present an approach which combines, for the first time, full asymptotic analysis with first-principles calculations based on the local-density approximation (LDA) of the density functional theory.

All theoretical models agree in the asymptotic form of the coupling for large spacer thickness:

$$J(D) = \frac{1}{D^2} \sum_i A_i \cos(Q_i D + \phi_i), \quad (1)$$

where D is the spacer thickness and A_i, Q_i, ϕ_i are the amplitude, the size of the corresponding extremal wave vector and the phase, respectively, for each oscillatory contribution. The first such model^{4,5} proposed for the OEC was based on the perturbative Ruderman-Kittel-Kasuya-Yosida (RKKY) theory for the interaction of isolated magnetic impurities in a nonmagnetic host metal. In the case of layered magnetic structures the role of the isolated impurities in the RKKY theory is played by the magnetic layers. Among other features $J(D)$ was found to be given by an integral over the wave vectors parallel to the layers \mathbf{k}_{\parallel} and, for large D , this was evaluated by the saddle-point method. Encouragingly, the result obtained displayed similarity with the experimental observations. In particular the oscillation periods predicted by the study of the Fermi surface of Cu fitted well to the observed oscillation periods for all the (100), (110), and (111) directions.^{5,7} Unfortunately, the same analysis is very complicated for complex Fermi surfaces such as the transition metal ones. Thus, for example, until recently, the large oscillation period for Cr spacer was an open question.^{37,38}

Theories based on more complete models, which emphasized the confinement of certain electrons to within the spacer was developed by Edwards *et al.*³³ and Stiles.³⁴ Usually, the models we have mentioned so far are based on a semiempirical tight-binding description of the electronic structure which facilitates the asymptotic analysis but intro-

duces the need to fit to either first-principles calculations or experiments. Alternatively, fully first-principles total-energy calculations offer a rather straightforward approach: The total energy of the system is calculated, using any electronic structure method, for the ferromagnetic as well as the anti-ferromagnetic orientation of the magnetic layer moments for a given spacer thickness and their difference corresponds to the OEC energy. While straightforward, the main disadvantages of total-energy calculations are the computational inefficiency and the obscurity in relating the OEC to the electronic structure of the spacer. In particular, it is not very efficient to take the Fourier transform of the calculated oscillatory coupling energy and compare the wavelengths of the dominant component with the Fermi-surface caliper vectors. Indeed, this procedure becomes unworkable for transition-metal spacers like Cr with complicated Fermi surfaces and thus a large number of nonequivalent caliper vectors with similar sizes.

From the computational point of view, the most difficult part of these total-energy calculations for layered structures is the two-dimensional Brillouin-zone integration. The advantage of the model approaches mentioned above is that this integration is considered in the asymptotic limit of large spacer thicknesses and only the neighborhood of a small number of k points contribute. Moreover, the asymptotic analysis defines the connection between the OEC and the extremal vectors of the Fermi surface of the bulk spacer. In the present paper we introduce an approach for the study of OEC based on the screened, layered KKR electronic structure method³⁹ and illustrate its use by explicit calculations for the Co/Cu/Co system mentioned above. In Sec. II, we summarize the theory as will be applied in the computational part of this work. In the Appendix, the theory is completed by the derivation of an analytic formula in the more general case of binary alloy spacers. Although that formula is not applied in this work we found it useful in Sec. IV. The linear phase approximation, the validity of which is examined in Sec. III, has also been introduced in the Appendix. The computational part of the present work is included in Sec. III, where we present our results for the OEC in the Co/Cu/Co trilayer system for all the (100), (110), and (111) orientations. The comparison of the asymptotic analysis results with the full integration ones and with experiments are also discussed in Sec. III. Finally, in Sec. IV we discuss how first-principles calculations based on asymptotic analysis, such as the ones in the present work, facilitate the use of the OEC measurements as a probe for the Fermi surface of random binary alloy spacers.

II. A KKR THEORY OF THE OSCILLATORY EXCHANGE INTERACTION

The reference structure considered in the following theoretical discussion is shown in Fig. 1. It consists of two semi-infinite layers of magnetic material which are separated by a nonmagnetic spacer of finite thickness D . A perfect structure is assumed, i.e., there is no lattice mismatch at the interfaces. Neither is surface roughness present. When desirable, the spacer could be optionally substitutionally disordered, consisting of two different kinds of atoms randomly distributed on a perfect underlying lattice.

Following the spirit of Ref. 40, we will start from a general expression for the LDA grand potential Ω in terms of the integrated density of states, which in the KKR and KKR-CPA formalism can be written in a particularly transparent form. Namely, we write

$$\begin{aligned}\Omega &= -\frac{1}{\beta} \left\langle \sum_{\nu} \ln(1 + e^{-\beta(\varepsilon_{\nu} - \mu)}) \right\rangle \\ &= \frac{1}{\pi} \text{Im} \int_{-\infty}^{\infty} dE f(E) \ln \|M^{(eff)}(E)\|,\end{aligned}\quad (2)$$

where we have neglected the double counting corrections.^{41,42} The first part of the above equation is a general definition of the grand potential in terms of the one-particle energy eigenvalues of the system ε_{ν} , the chemical potential, and the temperature T ($\beta = 1/K_B T$). The symbols $\langle \cdot \rangle$ and $\langle \cdot \rangle$ denote the averaging over all the configurations if the spacer is a random binary alloy. On the right-hand side we replaced $\langle \ln \|M\| \rangle$ by $\ln \langle \|M\| \rangle = \ln \|M^{(eff)}\|$ neglecting the so-called vertex corrections using the arguments of Velický.⁴³ The quantity $M^{(eff)}$ is an effective KKR matrix for the case where the necessary averaging is carried out employing the CPA. Also $f(E)$ is the Fermi-Dirac distribution function. The matrix $M^{(eff)}$ in the KKR-CPA theory⁴⁴ is given by

$$M^{(eff)} = [t^{(eff)}]^{-1} - G, \quad (3)$$

where, in the usual site, angular momentum, and spin representation, $t^{(eff)}$ is a single site scattering matrix and G is the structure constant matrix. The disorder in the case of the random binary alloy spacer is introduced through the effective $t^{(eff)}$ matrix which in the spacer region C in Fig. 1, is calculated within the CPA,⁴⁴ while in regions L and R it is the usual t -matrix describing the pure metal magnetic layers. A major disadvantage of the plain KKR method when applied to systems with reduced periodicity, such as layered structures, is the extended form of the structure constants. That problem was overcome in both LMTO and KKR methods by the recent screening revolution.³⁹ Thus, we will work in the screened representation³⁹ and the real-space structure constant matrix $G_{LL'}(\mathbf{R}_j - \mathbf{R}_i; E)$ will be assumed to be short ranged.

The screened form of $M^{(eff)}$ allows us to write it in the form

$$\begin{aligned}M^{(eff)} &= \begin{pmatrix} M_{LL} & M_{LC} & 0 \\ M_{CL} & M_{CC} & M_{CR} \\ 0 & M_{RC} & M_{RR} \end{pmatrix} = \begin{pmatrix} M_{LL} & 0 & 0 \\ 0 & M_{CC} & 0 \\ 0 & 0 & M_{RR} \end{pmatrix} \\ &\quad - \begin{pmatrix} 0 & G_{LC} & 0 \\ G_{CL} & 0 & G_{CR} \\ 0 & G_{RC} & 0 \end{pmatrix},\end{aligned}\quad (4)$$

where L , C , and R stand for the left, center, and right layers, respectively. Obviously, $M_{LR}, M_{RL} = 0$ due to the short-ranged form of the structure constants in the screened representation. For clarity we note that M_{LL} and M_{RR} are described by the pure metal t matrices: t_L^{-1} and $t_R^{(-1)}$ and M_{CC} corresponds to either a pure metal spacer described by t_C^{-1} or

an alloy described by t_{CPA}^{-1} . It should also be stressed that all the quantities in the above formula should be considered spin dependent, since we are interested in calculating the energy difference between parallel and antiparallel alignment of the magnetic layers. The purpose of the above, rather abstract, notation is to facilitate the separation of the relevant, D -dependent part of the Grand potential.^{41,42} To proceed with this goal, using Eq. (4), the logarithm of the determinant of M can be written as follows:

$$\begin{aligned}\ln \|M\| &= \text{Tr}\{\ln M_{LL}\} + \text{Tr}\{\ln M_{CC}\} + \text{Tr}\{\ln M_{RR}\} \\ &\quad + \text{Tr}\{\ln(1 - \tau_{CC}\Delta_L - \tau_{CC}\Delta_R)\},\end{aligned}\quad (5)$$

where $\Delta_L = G_{CL}\tau_{LL}G_{LC}$, $\Delta_R = G_{CR}\tau_{RR}G_{RC}$, while $\tau_{CC} = M_{CC}^{-1}$, $\tau_{LL} = M_{LL}^{-1}$, and $\tau_{RR} = M_{RR}^{-1}$. It is evident that the first three terms in Eq. (5) do not correspond to interactions between different slabs. Thus, substituting the expression of Eq. (5) in the integral of Eq. (2) we can concentrate only on the part coming from the only term which involves scattering on both sides of the spacer layer, namely the last term of Eq. (5). Of course, the isolated, single interface interactions between L and C slabs as well as C and R slabs are also included in the last term of Eq. (5) and should be separated off and left out of consideration due to the fact that we are interested in the interaction of L and R slabs only. To achieve this end, we write the last term of Eq. (5) in the form

$$\begin{aligned}\text{Tr}\{\ln(1 - \tau_{CC}\Delta_L - \tau_{CC}\Delta_R)\} \\ = \text{Tr}\{\ln(1 - \tau_{CC}\Delta_L)\} + \text{Tr}\{\ln(1 - \tau_{CC}\Delta_R)\} \\ + \text{Tr}\{\ln(1 - \tau_{CC}\hat{\Delta}_L\tau_{CC}\hat{\Delta}_R)\},\end{aligned}\quad (6)$$

where we have introduced the notation: $\hat{\Delta}_L = \Delta_L(1 - \tau_{CC}\Delta_L)^{-1}$ and $\hat{\Delta}_R = \Delta_R(1 - \tau_{CC}\Delta_R)^{-1}$. As shown in Ref. 39, the first two terms correspond to the single interface interactions and the third one is the one we will focus our interest. In this term the $\hat{\Delta}_L$ and $\hat{\Delta}_R$ are properties of the two interfaces of L and R layers with the C layer in the sense that they are localized around the interface. On the other hand, τ_{CC} is property of the spacer. Thus, at this point we can separate the L and R interaction and write it as

$$\delta\Omega_{LR} = \frac{1}{\pi} \text{Im} \int_{-\infty}^{\infty} dE f(E) \text{Tr}\{\ln(1 - J(E))\}, \quad (7)$$

with $J(E) = \hat{\Delta}_L\tau_{CC}\hat{\Delta}_R\tau_{CC}$. Note that the formal expression in Eq. (7) allows us to compute the interaction energy directly instead of as a difference between two large total energies. Hence, it is in itself a significant step forward. However, we shall carry the analytic considerations still further before we begin numerical computations. Clearly, to evaluate the Tr operation in Eq. (7) a plane by plane representation is the most convenient, since all the quantities have two-dimensional translational invariance. Also the principal layers formulation introduced in Refs. 39,45 will be adopted. Within that formulation the atomic planes are grouped together into the so-called principal layers of varying size and the structure constants matrix elements are nonzero only between neighboring principal layers. Thus, we can write

$$[G_{CL}]_{P,Q} = G_{10}\delta_{P,1}\delta_{Q,0}, \quad [G_{LC}]_{P,Q} = G_{01}\delta_{P,0}\delta_{Q,1},$$

$$[G_{RC}]_{P,Q} = G_{01}\delta_{P,N}\delta_{Q,N+1}, \quad [G_{RC}]_{P,Q} = G_{10}\delta_{P,N+1}\delta_{Q,N}, \quad (8)$$

where P, Q are the principal layer indices. The convention adopted for principal layers indexing is shown in Fig. 1. The Δ_L and Δ_R as well as $\hat{\Delta}_L$ and $\hat{\Delta}_R$ are localized at the layers with indices 1 and N , respectively. As a consequence the matrix element of J in the plane-by-plane representation is

$$[J]_{P,Q} = \hat{\Delta}_L[\tau_{CC}]_{1,N}\hat{\Delta}_R[\tau_{CC}]_{N,Q}\delta_{P,1}. \quad (9)$$

As a next step, we approximate the logarithm in Eq. (7) by its first-order power series expansion in J . This approximation is valid for large N , since in Eq. (9) nondiagonal matrix elements of τ contribute to J and these are also expected to be small due to screening. The interaction grand potential $\delta\Omega_{LR}$ now becomes

$$\delta\Omega_{LR} = \frac{1}{\pi} \int_{-\infty}^{\infty} dE f(E) \frac{S}{(2\pi)^2} \int_{(SBZ)} d^2\mathbf{k}_{\parallel} \times \text{Tr}\{\hat{\Delta}_L[\tau_{CC}]_{1,N}\hat{\Delta}_R[\tau_{CC}]_{N,1}\}, \quad (10)$$

where the \mathbf{k}_{\parallel} integration is taken over the first surface Brillouin zone (SBZ), S is the real space area per surface unit cell, and finally Tr stands for the trace over the omitted indices like the spin and angular momentum.

The derivation of an analytic formula for the OEC in the general case of a binary alloy spacer is continued in the Appendix. The same derivation has also been presented in Ref. 40 and we included it in the Appendix with more detail for completeness and future reference. We also note that similar formulas have been derived by Dederichs *et al.*⁵³ but without the full first-principles treatment of all three components of the sandwich structure. In the remainder of this section we will present the formal details of the scheme we used in our actual calculations. In brief, the expression of Eq. (10) was evaluated either fully numerically, or by approximating the surface Brillouin zone integration by asymptotic estimate using the stationary phase method.^{46,47}

The calculation of $\hat{\Delta}_L, \hat{\Delta}_R$ requires the calculation of τ_{LL} and τ_{RR} which in the case of screened KKR can be performed for the required semi-infinite geometry using iterative techniques.³⁹ By contrast, the inversion of M_{CC} for the spacer slab is a straightforward inversion since the matrix has finite thickness. In the Appendix we show how $(\tau_{CC})_{1,N}$ can be evaluated in the $D \rightarrow \infty$ limit, using the formula that will be given in Eq. (A1).

In order to calculate the integral over E in Eq. (10) the Matsubara poles technique was used for finite temperature $T=300$ K and in our case 5–10 Matsubara poles were found to be enough to achieve convergence. The remaining double integration over the surface Brillouin zone is computationally the most difficult task of our calculation. As we shall now discuss, we performed that integration both numerically and using asymptotics.

In order to introduce the asymptotic stationary phase

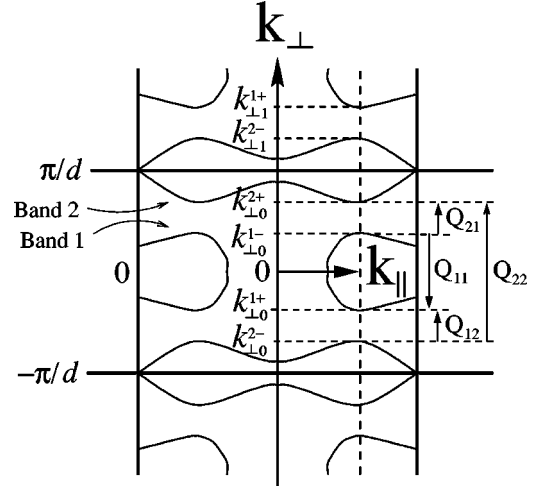


FIG. 2. Schematic view of a cut of the surface defined by $E_{\mathbf{k}} = E$ in the repeated zone scheme, with the poles $k_{\perp m}^{\nu\pm}$ encountered in the k_{\perp} integrations of Eq. (A2). For $E = E_f$, where E_f is the Fermi energy, we have a cut of the bulk spacer Fermi surface. The spanning vectors $Q_{\nu\nu'} = k_{\perp m}^{\nu+} - k_{\perp m}^{\nu'-}$ are also shown for a particular \mathbf{k}_{\parallel} for which they are extremal.

method to evaluate the integral over \mathbf{k}_{\parallel} in the surface Brillouin zone we have recast $\delta\Omega_{LR}$ of Eq. (10), in the Appendix as follows:

$$\delta\Omega_{LR} = \int_{(SBZ)} d^2\mathbf{k}_{\parallel} \sum_{\nu\nu'} h_{\nu\nu'}(\mathbf{k}_{\parallel}) \cong \int_{(SBZ)} d^2\mathbf{k}_{\parallel} \sum_{\nu\nu'} g_{\nu\nu'}(\mathbf{k}_{\parallel}) e^{iQ_{\nu\nu'}(\mathbf{k}_{\parallel})D}, \quad (11)$$

where the general integrand $h_{\nu\nu'}(\mathbf{k}_{\parallel})$ has been approximated by the form $g_{\nu\nu'}(\mathbf{k}_{\parallel})\exp[iQ_{\nu\nu'}(\mathbf{k}_{\parallel})D]$ amenable to an application of the saddle-point method. Moreover, the indices ν, ν' label the different branches of the Fermi surface and the wave numbers $Q_{\nu\nu'}(\mathbf{k}_{\parallel})$ are assumed to be spanning vectors of the Fermi surface of the bulk spacer connecting the ν, ν' branches (see Fig. 2). As explained in the Appendix the form of the phase $Q_{\nu\nu'}D$ is the consequence of the linear phase approximation responsible for involving the bulk spacer Fermi surface. The validity of this approximation has been tested explicitly by comparing the phases of the integrand to the extremal vectors of the bulk spacer Fermi surface multiplied by the spacer thickness. Integrals such as the ones in the right-hand side of Eq. (11) have the advantage that an analytic result for the integral can be written for the spacer thickness $D \rightarrow \infty$. The fact that $Q_{\nu\nu'}(\mathbf{k}_{\parallel})$ are real for pure spacers makes it convenient to use the stationary phase method instead of the more general saddle-point method we employed in the Appendix, where spacer disorder is taken into account. Following the standard stationary phase method^{46,47} the main contribution to the integral of Eq. (11) comes from the neighborhoods of points $\mathbf{k}_{\parallel}^{(\mu)}$ where $Q_{\nu\nu'}(\mathbf{k}_{\parallel})$ becomes stationary. Expanding $Q_{\nu\nu'}(\mathbf{k}_{\parallel})$ about one such stationary point to second order in $\mathbf{k}_{\parallel} - \mathbf{k}_{\parallel}^{(\mu)}$ and performing the corresponding Gaussian integral leads to the familiar result^{46,47}

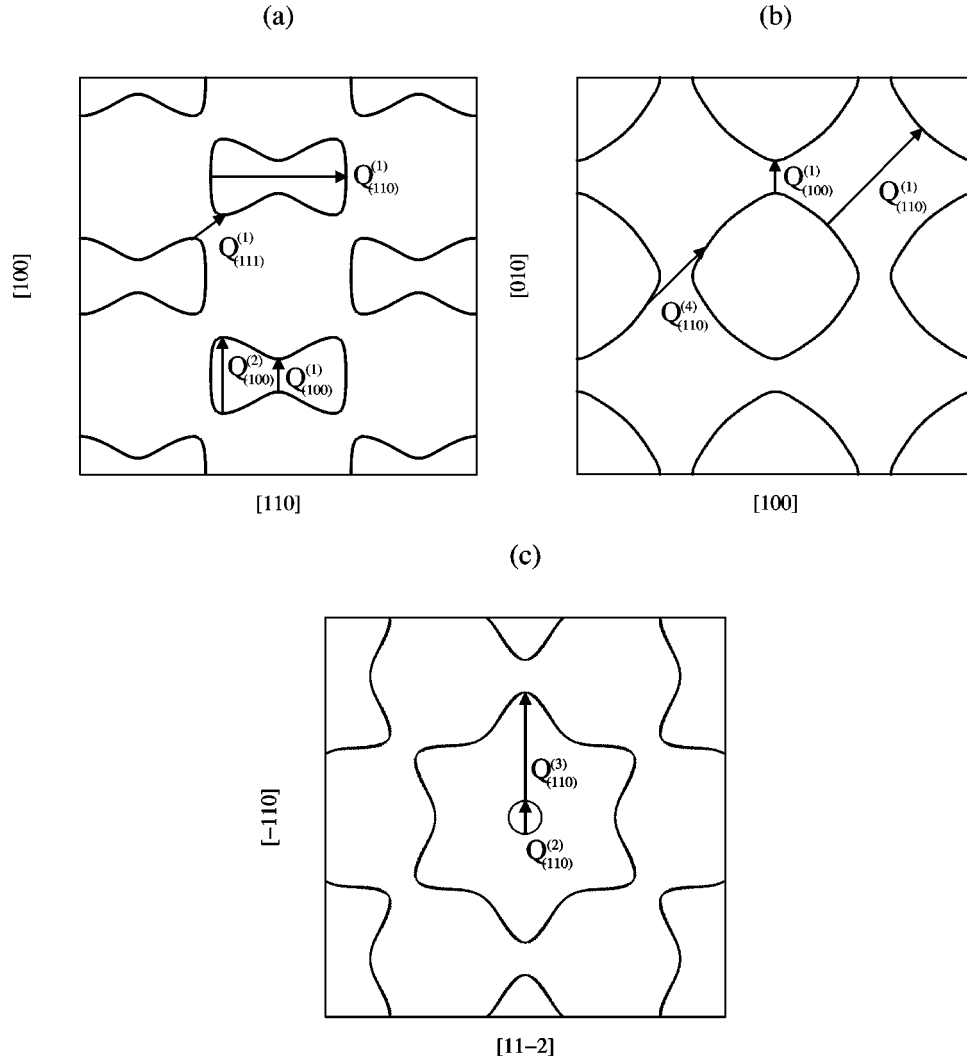


FIG. 3. The extremal vectors of Cu Fermi surface on three cuts plotted in the repeated zone scheme: a cut perpendicular to the [1-10] direction at a distance $\Delta k=0$ to the Γ point (a), perpendicular to the [001], $\Delta k=0$ (b) and perpendicular to the [111], $\Delta k=\sqrt{3}/2$ (c).

$$\int_{(SBZ)} d^2 \mathbf{k}_{\parallel} h_{\nu\nu'}(\mathbf{k}_{\parallel}) \cong \frac{2\pi\nu h^{(\mu)}}{D\sqrt{|\xi_1\xi_2|}} \quad \text{with}$$

$$\nu = \begin{cases} 1 & \text{for } \xi_1\xi_2 < 0 \\ i & \xi_1, \xi_2 > 0 \\ -i & \xi_1, \xi_2 < 0, \end{cases} \quad (12)$$

where $h^{(\mu)}$ is the value of the integrand at the extremal point $\mathbf{k}_{\parallel}^{(\mu)}$ and ξ_1, ξ_2 are the eigenvalues of the second derivative matrix of $Q_{\nu\nu'}$ at the extremal point. Apparently $h^{(\mu)}$ is an oscillatory function of D with a corresponding wave vector equal to the size of the μ th extremal vector. The difficulty in applying the stationary phase method is that it requires the search for the stationary spanning vectors of the Fermi surface of the spacer, which in cases such as the transition-metal spacers is fairly complicated. In addition, it requires the evaluation of the second derivative matrix of these vectors at the extremal points. However, this is a small price to pay for having avoided the necessity of a computationally even more demanding \mathbf{k}_{\parallel} integration. Moreover, the result relates the

OEC directly to the extremal spanning vectors of the Fermi surface and thereby identifies the physical causes of the oscillations.

III. RESULTS AND DISCUSSION

In this section we report our calculations of the OEC for all three principal orientations, (100), (110), and (111), for the Co/Cu/Co system. In Fig. 3, different cuts of the Cu Fermi surface, which was calculated with the KKR method, are shown and the extremal vectors have also been included for easy reference.

A. (100) orientation

There are two different extremal vectors along (100) direction, namely, the $Q_{(100)}^{(1)}$ and $Q_{(100)}^{(2)}$, shown in Fig. 3(a), spanning the so-called ‘‘dogs bone.’’ The corresponding oscillation periods, predicted from the Fermi surface which was calculated using the KKR method for the bulk spacer, are 6.3 and 2.5 ML, respectively. In Fig. 4 we report our results for the OEC energy as a function of spacer thickness. In Fig. 4(a) we compare the results of computing the two-

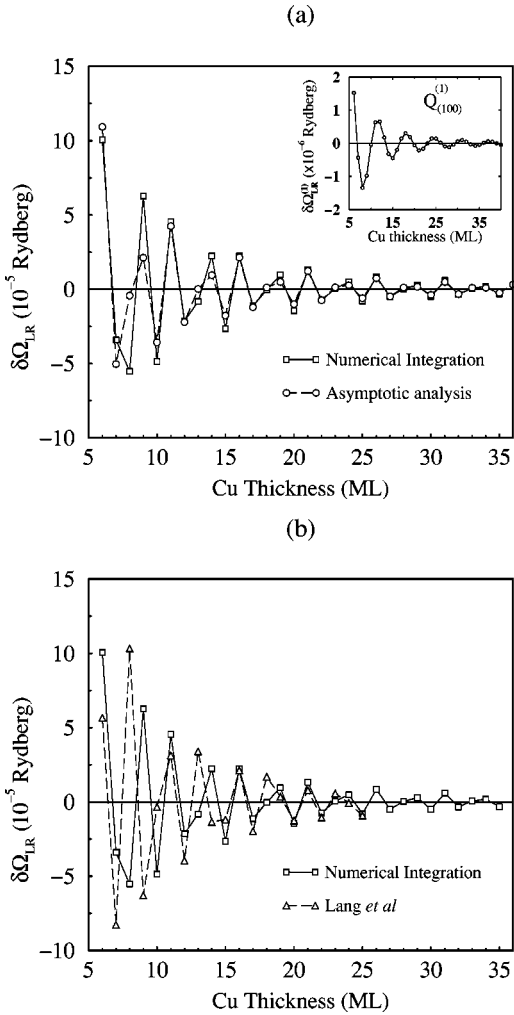


FIG. 4. Calculated OEC energy per surface atom ($\delta\Omega_{LR}$) for Co/Cu/Co(100) as a function of Cu spacer slab thickness. Comparison of the numerical integration with the asymptotic analysis results is shown in (a), while in (b) comparison between the numerical integration result of the present work and the calculations of Lang *et al.*, (Ref. 12) is shown. The contribution $\delta\Omega_{LR}$ originating from $Q_{(100)}^{(1)}$ is shown in the inset in (a).

dimensional \mathbf{k}_{\parallel} integration fully and that obtained by evaluating the formulas derived by the stationary phase, asymptotic method. In the stationary phase calculation only $Q_{(100)}^{(2)}$ was used since the contribution from the $Q_{(100)}^{(1)}$ is negligible. In fact the contribution from the stationary vector $Q_{(100)}^{(2)}$ was found to be two orders of magnitude smaller than the small period oscillation. To be yet more precise, at 6 ML of Cu thickness, where we have an AF peak for both contributions, the energy ratio was 67. Clearly, the stationary phase method results are in satisfactory agreement with the numerical integration for spacer thickness $D \geq 15$. Reassuringly, concerning the amplitude of the OEC energy there is also agreement with experiment. In particular, Johnson *et al.*¹⁹ have measured 0.4 mJ/m^2 for the OEC energy for an average spacer thickness 6.7 ML. Our values for 6 ML (10.8 Å) and 7 ML (12.6 Å) are significantly higher, being 3.3 and -1.0 mJ/m^2 , respectively. However, in other measurements on samples prepared differently the deduced values can be significantly different.⁴⁸ As we have already men-

tioned, the (100) is the most theoretically studied orientation for the Co/Cu/Co system. In Fig. 4 we compare our numerical integration result with the calculation of Lang *et al.*¹² The agreement is rather remarkable if we consider the fact that although the KKR method was also used in Ref. 12, the whole approach is different and is based on embedding a finite number of ferromagnetic layers in bulk Cu host. The agreement is improved for large spacer thickness as seen in Fig. 4(b). There is also agreement with the semiempirical calculations of Lee *et al.*,¹⁶ where a coupling strength of 6.7 mJ/m^2 is reported for 10 Å of Cu spacer thickness. This compares well with our value for 6 ML (10.8 Å).

B. (110) orientation

From the point of view of the oscillatory coupling this is the most complicated orientation since four different extremal vectors $Q_{(110)}^{(1)}$, $Q_{(110)}^{(2)}$, $Q_{(110)}^{(3)}$, and $Q_{(110)}^{(4)}$ (Fig. 3) are found to contribute.^{7,16,17} The corresponding oscillation periods, predicted from the bulk Fermi surface calculation, are 2.07, 10.4, 2.5, and 3.2 ML, respectively. The first one corresponds to the belly diameter which is equivalent, due to the aliasing effect, to the “dogs bone” length, while the second of these extremal vectors correspond to the Fermi surface neck diameter along the (110), as shown in Fig. 3. This is the only one that originates a long period oscillation. The contribution from $Q_{(110)}^{(1)}$ and $Q_{(110)}^{(2)}$ extremal vectors were found to dominate the OEC as shown in Fig. 5. The amplitude of the short period oscillation is the largest one, but the contribution from $Q_{(110)}^{(2)}$ is also significant as can be seen in Fig. 5. Evidently, the sum of the stationary phase contributions is significantly larger in size than the full numerical result for relatively small Cu slab thicknesses and the convergence is achieved only for approximately 40 ML thickness. By contrast, for the phase, convergence is achieved for very small spacer thickness (10 ML). The effect of late convergence of the amplitudes can be explained by the relatively flat Fermi surface in the neighborhood of the endpoints of the $Q_{(110)}^{(1)}$ extremal vector. Apparently, the quadratic expansion of the exponent which leads to the result of the stationary phase method⁴⁷ is not enough for this case and higher order corrections⁴⁹ are necessary for relatively small spacer thicknesses. It is clearly a puzzle that the long period oscillation is the only one seen experimentally although its strength in the calculation appears to be much smaller. There are no reports so far for the short period, which is approximately two monolayers long and is almost commensurate with the layers. At this stage of theory, one cannot but argue that such short period oscillations are destroyed by interfacial disorder. While this is a plausible explanation,¹³ the subject deserves further scrutiny. Focusing our attention to the short period contribution (Fig. 5), the agreement with the experimental amplitudes is restricted to the order of magnitude: 0.7 mJ/m^2 is the experimental value¹⁹ for the first AF peak, while our calculated one is 1.8 mJ/m^2 . On the other hand, there is fairly good agreement with the KKR calculation result of Nordstrom *et al.*¹³ in both the amplitudes and periods. Interestingly, Nordström *et al.* simulated the effect of surface roughness for the [110] orientation and observed the smearing out of the small period oscillation in agreement with experiments and despite the fact that in their calculation, as

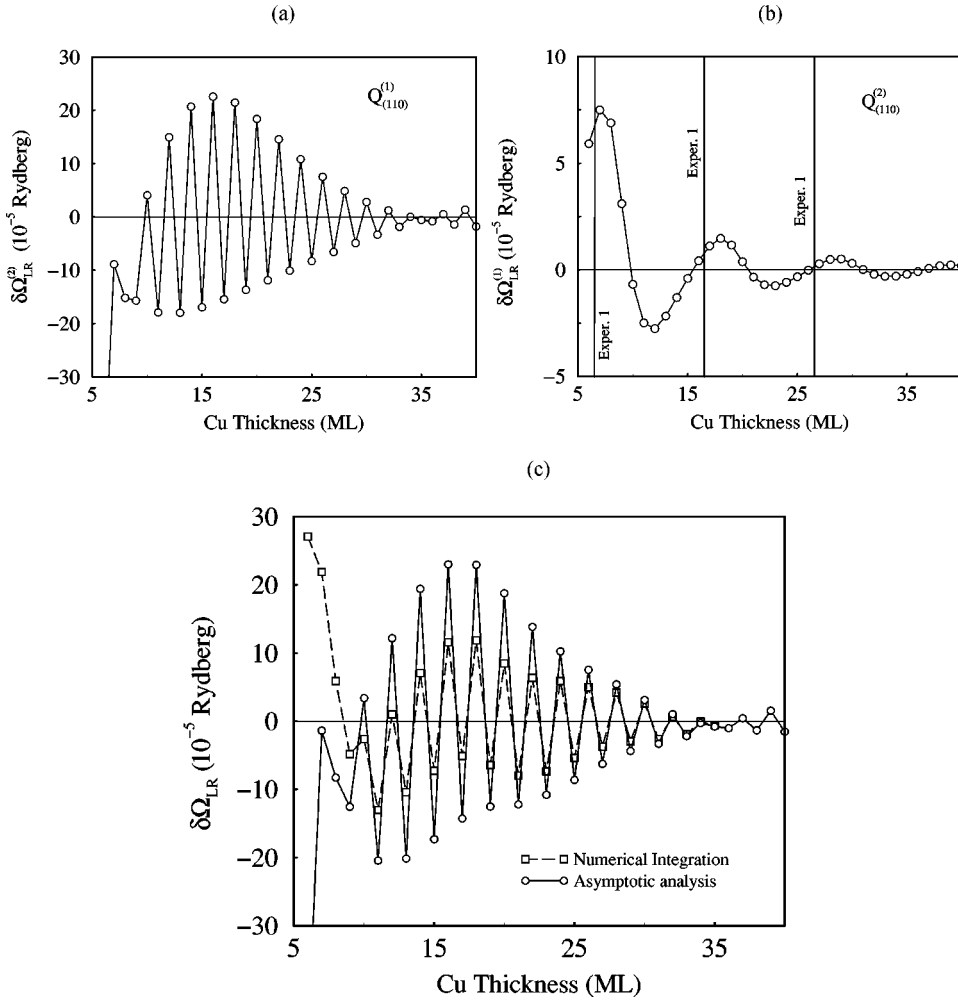


FIG. 5. The contributions $\delta\Omega_{12}^{(1)}$, $\delta\Omega_{12}^{(2)}$ to the interaction energy $\delta\Omega_{12}$ arising from the $Q_{(110)}^{(1)}$ (a) and the $Q_{(110)}^{(2)}$ (b) extremal vectors, and the comparison of the total asymptotic analysis result with that of the full numerical integration (c). The vertical lines in (b) marked with (Exper. 1) correspond to the position of the AF peaks found in the experiment of Johnson *et al.* (Ref. 19).

in ours, the small oscillation is the dominant for the perfect structure. To be more specific, the position of the AF peaks they found in the case of rough surfaces are in agreement with experiment. Our result for the large period shows similar agreement, as seen in Fig. 5(b) where the vertical lines indicate the positions of the experimental AF peaks. The slight shift towards larger spacer thicknesses in our result is due to a small difference in the period and a small shift of the first AF peak. It is also noteworthy that the result of Nordström *et al.* for the rough surface seems to be slightly closer to the experiment than our result for the large oscillation contribution. In addition, the size of the first AF peak for the rough surface result of Nordström *et al.* is approximately four times larger than our large period oscillation. We believe that these differences are consequences of the fact that the small period oscillation is still contributing especially for the small spacer thicknesses. Indeed, our stationary phase result for perfect interfaces and isolating the large period contribution cannot be directly compared to their result, where the smearing out the small period oscillation was a result of simulating the interface roughness.

C. (111) orientation

For this orientation there is only one extremal vector $Q_{(111)}^{(1)}$. It spans the neck of the Fermi surface at an angle of 19.47° as can be seen in Fig. 3(a) and corresponds to an oscillation period of 5.0 ML size. Being the only case where

only one extremal vector exists, the (111) orientation is ideal for comparison between both the stationary phase result and the full numerical result with experiment. In Fig. 6 we again compare the stationary phase result with the full numerical result. In the same figure the positions of the experimental AF peaks are marked by vertical lines for two different experiments.^{19,50} Clearly, theory and experiments are in

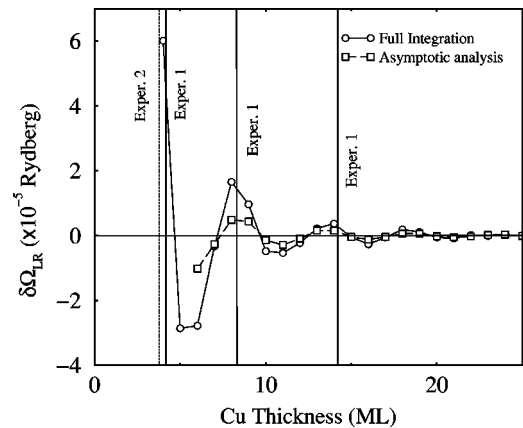


FIG. 6. The calculated OEC energy per surface atom $\delta\Omega$ for Co/Cu/Co(111) as a function of Cu spacer slab thickness. The position of experimental AF peaks is indicated by the vertical lines and correspond to experiments of Johnson *et al.* (Ref. 19) (Exper. 1) and Parkin *et al.* (Ref. 50) (Exper. 2).

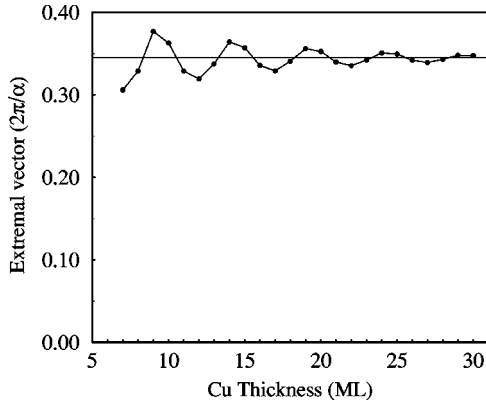


FIG. 7. The $Q_{(111)}^{(1)}$ extremal vector calculated using the KKR method for bulk Cu (horizontal line) compared with the value obtained from the phase of the integrand in the numerical integration over \mathbf{k}_{\parallel} as function of spacer thickness. In the limit of infinite spacer thickness the two values are equal and the linear phase approximation exact.

markably good agreement. We believe that the better agreement with experiment for the (111) case, compared to the (110), is due to the fact that only one period is present. Again, let us compare the amplitudes to experiment: for 4 ML the OEC energy has been measured by Johnson *et al.* and was found 1.1 mJ/m^2 , while our calculated value is 2.1 mJ/m^2 for the same spacer thickness.

For the case of (111) orientation we also examined the question: to what extent the linear phase approximation, delineated in the Appendix, is valid? In particular we examined the dependence on D of the phase of the integrand in the \mathbf{k}_{\parallel} integration evaluated at the extremal point for that orientation, i.e., at that \mathbf{k}_{\parallel} where $k_{\perp} = Q_{(111)}^{(1)}$ occurs. More specifically we compared the wave vector that comes from the integrand and the extremal vector obtained by a separate Fermi-surface calculation for the bulk spacer using the same atomic KKR potential and the bulk KKR code. A difficulty in finding the wave vector from the integrand is of course the selection of the correct branch of the logarithm of the complex integrand. Nevertheless, the result is shown in Fig. 7. As we see the wave vector obtained from the integrand is close to the extremal vector size and the agreement is rapidly improved as the number of spacer layers is increased. Indeed, the linear phase approximation is exact at $D \rightarrow \infty$ as pointed out in the Appendix, but we see that even for relatively small thicknesses the size of the fluctuations is small compared to the absolute value of $Q_{(111)}^{(1)}$. Anyway, as our results indicate, roughly speaking, the Fermi surface extremal vectors agree well with the oscillation periods of the OEC, but when more accurate measurements of the OEC energy become available deviations from the linear phase approximation should definitely be taken into account in addition to higher-order corrections in the stationary phase expansion.⁴⁹ Nevertheless, given the present state of the experiments, the fact that the phase of the integrand oscillates about the linear increase $Q_{(111)}^{(1)}D$ does not prevent us from comparing, successfully, the OEC periods to the bulk spacer Fermi surface extremal vectors even if the experiments correspond to small spacer thicknesses.

IV. MEASURING THE FERMI SURFACE

Summing up the results of the OEC over the past 10 years^{7,53} including those reported in the present paper, we may conclude that the evidence for the effect being a direct, quantitative consequence of the Fermi surface is overwhelming. Thus having illuminated the physical origin of the oscillatory exchange coupling, perhaps it is time to turn around and use the measurements of the OEC to learn about the geometry of the Fermi surface. This point of view lends particular relevance to the subject matter of the present paper. Evidently, the reconstruction of the Fermi surface from measurements of the OEC requires the accomplishment of two separate tasks: the first is that of deducing the size and orientation of the extremal wave vectors $Q_{(\alpha\beta\gamma)}^{(\mu)}$ from the measurements and the other is a construction of the Fermi surface from a collection of measured extremal wave vectors. Here we wish to comment only on how our results further the cause of the former. The main point to consider is this: only theories which are based on an asymptotic analysis like ours and give the OEC as separate contributions from the specific calipers of the Fermi surface are useful in the interrogation of the experimental data with the above purpose in mind, and to be effective, the confrontation between the data and theory will involve the theoretical determination of phases and the amplitudes as well as the periods of the individual oscillations. The principle achievement of the present paper is to provide a first-principles and, therefore, parameter-free prescription for calculating all three of these quantities on the same footing. This result is encapsulated in Eq. (A7). As a scrutiny of this formula reveals, the amplitudes and phases depend not only on the curvature of the Fermi surface near the endpoints of the extremal wave vectors, but also on a full self-consistent first-principles description of the magnetic layer-spacer layer interface through the quantities Δ . Thus, our calculation takes into account the material specific nature of the interface using the same LDA crystal potential far from the interface as is used for the Fermi-surface calculation. Clearly, this consistent treatment of the magnetic layers, spacer layers, and the interface between them is necessary if we are to calculate reliably the relative contributions from each of the extremal wave vectors.

Note that Eq. (A7) is an analog of the Lifshitz-Kosevich formula (Ref. 51), which is commonly used to interpret de Haas-van Alphen (dHvA) oscillations in terms of Fermi-surface cross-sectional areas. Clearly, because of the significant role played by the interface and the orders of magnitudes higher accuracy of the dHvA experiments, measurements of the OEC are not likely to compete with the results of the former in pure metals. However, in the case of random alloys where dHvA becomes ineffective, due to the requirement of long lifetimes, experimental determination for the OEC may have an important role to play. Here, 2D-ACAR experiments⁵² are the only competitors to OEC measurement as a new probe of the Fermi surface. To some extent the present work was undertaken in the hope that in this role the study of OEC may lead to significant progress.

It is to make the above point that we have presented, in the Appendix, a generalized version of the otherwise more or less conventional, asymptotic analysis which is applicable

when the stationary points of the integrand in Eq. (11) is in the complex plane. As a result we find that for alloy spacers

$$J(D) = \frac{1}{D^2} \sum_{\nu} A_{\nu} \cos(Q_{\nu}D + \phi_{\nu}) e^{-(D/\Lambda_{\nu})}. \quad (13)$$

As before, in addition to the periods the KKR-CPA theory determines both the amplitudes and the phases. Clearly, the qualitative new feature of Eq. (13) is the exponential decay. Thus, one expects to observe OEC only for spacer thicknesses $D < \Lambda_{\nu}$. Fortunately, the KKR-CPA theory also provides an unambiguous, quantitative answer for Λ_{ν} . As explained in the Appendix, it is related to the width of the spectral function $A_{\beta}(\mathbf{k}, E)$ at the endpoints of the extremal wave vectors Q_{ν} . So far, these decay constants have been evaluated only for two alloy spacers.^{17,18,38} Both in the case of $\text{Cu}_{(1-x)}\text{Ni}_x$ for $x \leq 0.42$ and $\text{Cr}_{(1-x)}\text{V}_x$ alloys Λ was found to be much larger than the thickness of the spacers in the experimentally investigated structures. Thus, no exponential cutoff was expected and encouragingly, none was found in these experimental studies^{17,20,54,55} of cases where $D \leq \Lambda_{\nu}$. Here we digressed to consider the effect of disorder only to point out that in the case of random alloys, whose Fermi surface is most likely to be studied with profit by measuring the OEC and the KKR-CPA based asymptotic analysis, the method we have presented in this paper, will also provide an account of the observability of the OEC.

V. CONCLUSION

In conclusion, a first-principles theoretical method, based on the KKR and KKR-CPA description of the electronic structure and an asymptotic analysis technique was presented in full detail for the study of the oscillatory exchange coupling of two ferromagnetic layers across a nonmagnetic spacer which could optionally be a pure metal or a random binary alloy. The use of the saddle-point asymptotic technique resulted, on the one hand, in a much faster computation of Brillouin-zone integrals over \mathbf{k}_{\parallel} vectors parallel to the layers technique and on the other hand, in an explicit decomposition of the OEC into contributions arising from the extremal vectors of the Fermi surface. The method was used for the study of the Co/Cu/Co trilayer system for all the (100), (110), and (111) orientations and the obtained results were found to be in satisfactory agreement with experiments and other calculations, both first principles and semiempirical, concerning all the coupling characteristics, i.e., the periods, amplitudes, and phases. Some of the details of the method, such as the linear phase approximation which is crucial in all theoretical approaches of this kind in connecting the oscillations with the bulk spacer Fermi surface, were also tested in realistic calculations. OEC is proven to be a powerful probe of the Fermi surface of random binary alloys, for which the dHvA oscillations technique fails. Certainly, from this point of view it is clear that a first-principles technique for interpreting OEC experiments is required, and our method serves that need.

ACKNOWLEDGMENTS

The authors would like to thank B. Ginatempo and E. Bruno from the University of Messina, for providing us with

the bulk KKR-CPA code developed by them and for their help on the implementation and use of the code. N.N.L. had financial support from the TMR network on ‘‘Interface Magnetism’’ (Contract No. ERBFMRXCT960089) of the European Union. Also B.U. was partly supported by the Hungarian National Science Foundation (OTKA T2 2609). Finally, B.L.G. would like to thank the Insitute of Theoretical Physics at the University of California–Santa Barbara for the hospitality during the preparation of this manuscript.

APPENDIX

In this appendix the derivation of an analytic formula for the OEC will be presented based on the KKR description of the electronic structure. More specifically, we shall establish a relationship, used in Sec. II, between the Fermi-surface characteristics of the infinite, bulk spacer and the asymptotic form of the OEC. As one might have expected, the properties of the single interface will also be involved, through the $\hat{\Delta}$ matrices introduced in Sec. II, in determining the amplitudes and phases of the OEC.

Let us begin with Eq. (10) and introduce our first major approximation, namely the assumption that the phase of the integrand is a linear function of D . Note that this approximation is crucial for all the theoretical models relating the Fermi surface of the bulk spacer material to the OEC periods. In our formalism this approximation is expressed as

$$[\tau_{CC}]_{1,N} \cong \frac{d}{2\pi} \int_{-\pi/d}^{\pi/d} dk_{\perp} e^{-ik_{\perp}(1-N)d} \tau_C(\mathbf{k}_{\parallel} + \mathbf{k}_{\perp}). \quad (A1)$$

In the above expression d is the principal layer spacing and $\tau_C(\mathbf{k})$ is the inverse KKR matrix for the infinite spacer in k space (complete lattice Fourier transform). In short, we approximate the $[\tau_{CC}]_{1,N}$ for the finite spacer, with $[\tau_C]_{1,N}$ for the infinite spacer. This approximation introduces the simple exponential form with the phase linear in the spacer thickness which will give rise to the oscillatory behavior as we will now demonstrate. The validity of this approximation examined in Sec. III for the trilayer Co/Cu/Co(111). Substituting the expression of Eq. (A1) in Eq. (10) we have the expanded expression

$$\begin{aligned} \delta\Omega_{LR} = & -\frac{1}{\pi} \text{Im} \int_{-\infty}^{\infty} dE f(E) \frac{S}{(2\pi)^2} \int_{SBZ} d\mathbf{k}_{\parallel}^2 \frac{d}{2\pi} \int_{-\pi/d}^{\pi/d} dk_{\perp} \\ & \times \frac{d}{2\pi} \int_{-\pi/d}^{\pi/d} dk'_{\perp} e^{i(k_{\perp} - k'_{\perp})(N-1)d} \text{Tr}_a \{ \mathcal{J} \}, \end{aligned} \quad (A2)$$

where

$$\begin{aligned} \mathcal{J}(E; \mathbf{k}_{\parallel}; k_{\perp}, k'_{\perp}) = & \hat{\Delta}_L(E; \mathbf{k}_{\parallel}) \tau_C(E; \mathbf{k}_{\parallel} + \mathbf{k}_{\perp}) \\ & \times \hat{\Delta}_R(E; \mathbf{k}_{\parallel}) \tau_C(E; \mathbf{k}_{\parallel} + \mathbf{k}'_{\perp}). \end{aligned}$$

At this stage it should be stressed that within the plane-by-plane representation its more convenient to redefine the k -space unit cell over which the integrations are carried out. Thus we have selected a prism with the base being the surface of the first Brillouin zone and the height equal to $2\pi/d$,

where d is the real-space neighboring plane distance.⁵⁶ With this definition of the unit cell the limits of the k_{\perp} integrations do not depend on \mathbf{k}_{\parallel} , while the \mathbf{k}_{\parallel} integration is extended over the surface Brillouin zone corresponding to the orientation of interest.

In what follows we will calculate the integrals in Eq. (A2). In brief, the integrations over k_{\perp} will be carried out using Cauchy's theorem and the spanning vectors along the k_{\perp} direction of the surface $E_{\mathbf{k}}=E$ for given E will be introduced. Next, the two-dimensional integration over the surface Brillouin zone will be calculated asymptotically, for spacer thickness tending to infinity, using the saddle-point asymptotic method and the extremal spanning vectors will be picked up. Finally, the integration over the energy will be done also employing asymptotic analysis and E will be restricted to the Fermi energy E_f only. Thus, at the end, a final formula will be derived where the extremal spanning vectors of the bulk spacer Fermi surface will be involved as well as the Fermi-surface curvature at the end points of the spanning vectors. All the quantities needed to calculate the periods, amplitudes and phases of the oscillations depending on E , \mathbf{k}_{\parallel} , and k_{\perp} will have to be computed only at the end-points of the extremal spanning vectors.

Apparently, due to the translational invariance of τ_C , the integrations over k_{\perp} and k'_{\perp} can be extended by any number of periods ($2\pi/d$) as long as the integral is normalized, i.e., divided by the length over which the integral is taken. This maneuver makes the Cauchy theorem applicable for evaluating these integrals. Consequently, for the integration over k_{\perp} we will consider a closed contour consisting of the real axis and the infinite radius semicircular path on the positive imaginary part half-plane, thus encountering only the poles with positive imaginary part. On the other hand for the integration over k'_{\perp} we should consider the semicircular path on negative imaginary part half-plane, i.e., encountering the negative imaginary part poles. As is well known,⁴⁴ the poles of the τ matrix correspond to the zeros of the KKR determinant for the infinite spacer, i.e., for these k_{\perp} , for given E and \mathbf{k}_{\parallel} that the dispersion relation $E_{\mathbf{k}_{\parallel}+\mathbf{k}_{\perp}}=E$ is satisfied. Since the integration limits are taken to infinity the poles in the repeated zone scheme should be considered. A schematic view of the location of these poles is shown in Fig. 2. Each pole in the 0th unit cell is labeled by $k_{\perp 0}^{\nu\pm}$, with ν being the band index. There are pairs of poles due to the reflection symmetry and \pm stands for a pair of such poles.

At this point, we would like to mention that the above poles are not on the real axis but are shifted into the complex k_{\perp} plane not only for disordered spacer materials but for pure materials as well. Let us define the complex poles by writing

$$g_{\perp m}^{\nu\pm} = k_{\perp m}^{\nu\pm} + iq_{\perp m}^{\nu\pm}, \quad (\text{A3})$$

where $q_{\perp m}^{\nu\pm}$ is the, as we shall argue, presently small imaginary part of the poles. In the case of pure spacer an infinitesimal imaginary part must be included in the energy argument of $\tau_C(E+is)$, where s is an infinitesimal positive number, as a matter of definition. Thus, even in this case, the poles are slightly shifted off the real axis. It could be easily seen that for each pole with an infinitesimal positive imaginary part there is one (its pair counterpart) with a negative

imaginary part. In the case of spacers with substitutional disorder, i.e., random binary alloy spacers, the poles move off the real axis by a finite amount and are given by an equation of the form

$$E - E_{\mathbf{g}_{\perp m}^{\nu\pm} + \mathbf{k}_{\parallel}} + i\Gamma(E; \mathbf{g}_{\perp m}^{\nu\pm} + \mathbf{k}_{\parallel}) = 0. \quad (\text{A4})$$

The fact that in the case of many binary alloy systems the Bloch spectral functions are very well fitted to Lorentzians, even for relatively large concentrations, suggests that Γ does not vary much with E in the neighborhood of the pole and taking it to be small is a good approximation. We will concentrate on the limit of small disorder and will regard Γ as a small quantity. Up to first order in Γ , we have that

$$g_{\perp m}^{\nu\pm} = k_{\perp m}^{\nu\pm} + i \frac{\Gamma(E; \mathbf{k}_{\perp m}^{\nu\pm} + \mathbf{k}_{\parallel})}{u_{\perp m}^{\nu\pm}}, \quad (\text{A5})$$

where $u_{\perp m}^{\nu\pm} = (\partial E_{\mathbf{k}} / \partial k_{\perp})_{k_{\perp m}^{\nu\pm}}$. Thus, the effect of disorder is again to add a small imaginary part to the pole defined by the real part of Eq. (A4) in perfect analogy to the nondisordered, pure spacer case. The difference is that for the case of pure spacers s is included for technical reasons and consequently both s and $q_{\perp m}^{\nu\pm}$ should go to zero at the end, while for binary alloys $q_{\perp m}^{\nu\pm}$ is a small but nonzero quantity, with physical meaning, resulting to an extra exponential dumping term. In Fig. 2 only the real part of these poles is shown. Finally, the poles are repeated in each unitary cell in the repeated zone scheme. Index m in $k_{\perp m}^{\nu\pm}$ in Fig. 2 stands for the m th unitary cell poles. Its also worth mentioning that the order of the pole is the band degeneracy number. In summary, the result of the k_{\perp} integration is

$$\begin{aligned} [\tau_{CC}]_{1N} &= id \sum_{\nu} W^{\nu+}(E; \mathbf{k}_{\parallel}) e^{g_{\perp m}^{\nu+}(N-1)d}, \\ [\tau_{CC}]_{N1} &= -id \sum_{\nu} W^{\nu-}(E; \mathbf{k}_{\parallel}) e^{-g_{\perp m}^{\nu-}(N-1)d}, \end{aligned} \quad (\text{A6})$$

where $W^{\nu\pm}(E; \mathbf{k}_{\parallel}) = \lim_{k_{\perp} \rightarrow g_{\perp 0}^{\nu\pm}} \{ \tau_{CC}(E; \mathbf{k}_{\parallel} + \mathbf{k}_{\perp})(k_{\perp} - g_{\perp 0}^{\nu\pm})^{\nu} \}$, i.e., the residue of τ_{CC} at the pole $g_{\perp 0}^{\nu\pm}$. After the integrations over k_{\perp} and k'_{\perp} the expression for the $\delta\Omega_{LR}$ takes the following form:

$$\begin{aligned} \delta\Omega_{LR} &= -\frac{1}{\pi} \sum_{\nu\nu'} \text{Im} \int_{-\infty}^{\infty} dE f(E) \frac{Sd^2}{(2\pi)^2} \\ &\quad \times \int_{SBZ} d^2\mathbf{k}_{\parallel} T_{\nu\nu'}(E; \mathbf{k}_{\parallel}) e^{iQ_{\nu\nu'}(E; \mathbf{k}_{\parallel})D}, \end{aligned} \quad (\text{A7})$$

where $D = Nd$ is the spacer thickness, $Q_{\nu\nu'} = g_{\perp 0}^{\nu+} - g_{\perp 0}^{\nu'-}$ are the spanning vectors between branches of the surface defined by $E_{\mathbf{k}}=E$ along the \mathbf{k}_{\perp} direction (see Fig. 2) and $T_{\nu\nu'} = e^{-iQ_{\nu\nu'}d} \text{Tr}\{\hat{\Delta}_L W^{\nu+} \hat{\Delta}_R W^{\nu'-}\}$. All the quantities $Q_{\nu\nu'}$, $\hat{\Delta}_L$, $\hat{\Delta}_R$, $W^{\nu+}$, $W^{\nu'-}$ are functions of \mathbf{k}_{\parallel} and E . Note that each of the quantities $Q_{\nu\nu'}$ is always a distance in the k_{\perp} direction between a pole with positive imaginary part and a pole with negative imaginary part. Another important issue is that an arbitrary number of $2\pi/d$ could be added to them. It

is convenient to select the smallest in size from these equivalent $Q_{\nu\nu'}$. This is a physical effect which gives rise to the aliasing effect.^{7,57}

Integrals of the form of Eq. (A7) can be evaluated analytically in the limit of infinite D using the standard saddle-point method also called method of steepest descent.^{46,47} In the case of pure metallic spacers we encounter the stationary points of the function $Q_{\nu\nu'}(E; \mathbf{k}_{\parallel})$, i.e., the stationary spanning vectors of the surface $E_{\mathbf{k}}=E$ on the real axis. In the case of disordered spacer $Q_{\nu\nu'}$ is complex ($Q_{\nu\nu'}=Q_{\nu\nu'}^R+iQ_{\nu\nu'}^I$). Nevertheless, in the limit of small disorder its imaginary part $Q_{\nu\nu'}^I$ is small and the problem remains tractable. Typically $Q_{\nu\nu'}^I$ is stationary at the points \mathbf{k}_{\parallel}^* where $Q_{\nu\nu'}^R$ is also stationary, i.e., $(\partial Q_{\nu\nu'}^I/\partial \mathbf{k}_{\parallel})_{\mathbf{k}_{\parallel}^*}=(\partial Q_{\nu\nu'}^R/\partial \mathbf{k}_{\parallel})_{\mathbf{k}_{\parallel}^*}=0$. This is a consequence of the fact that the extremal vectors are usually symmetry points connecting symmetric parts of the surface $E_{\mathbf{k}}=E$. Later E will be set equal to the Fermi energy, thus the surface will be the Fermi surface of the spacer. In the case of small disorder the Fermi surface of the bulk alloy is well defined by sharp peaks of the Bloch spectral function $A_B(\mathbf{k}, E_f)$ and thus it enters the calculation of the OEC in a manner similar to that in the case of pure metallic spacers.

To proceed with the saddle-point method let us define the function $G(\mathbf{k}_{\parallel})=iQ_{\nu\nu'}=G^R+iG^I$, with $G^R=-Q_{\nu\nu'}^I$ and $G^I=Q_{\nu\nu'}^R$, and investigate it in the neighborhood of the extremal point \mathbf{k}_{\parallel}^* . In order to calculate the integral over \mathbf{k}_{\parallel} in Eq. (A7) analytically we should consider the coordinates k_x , k_y in the \mathbf{k}_{\parallel} plane in such a way that the second derivative matrix of G is diagonal. One step further, we continue these variables to the complex plane, $g_x=k_x+iq_x$ and $g_y=k_y+iq_y$. Although the stationary vectors correspond to real \mathbf{k}_{\parallel} , the integration along the steepest descent direction involves G in the complex plane. Following the usual procedure^{46,47} for g_x and g_y independently we find

$$\delta\Omega_{LR}=\frac{Sd^2}{2\pi^2D}\sum_{\mu}\text{Im}\int_{-\infty}^{E_f}dE h^{(\mu)}(E)\exp[iQ^{(\mu)}(E)D],$$

where

$$h^{(\mu)}(E)=\frac{T^{(\mu)}e^{-i(\phi_x^{(\mu)}+\phi_y^{(\mu)})/2}}{\sqrt{|\xi_x^{(\mu)}\xi_y^{(\mu)}|}}. \quad (\text{A8})$$

The index μ enumerates the stationary points \mathbf{k}_{\parallel}^* for all the different pairs ν, ν' , so $T^{(\mu)}=T_{\nu\nu'}(\mathbf{k}_{\parallel}^*)$. The $\xi_x^{(\mu)}$

$=|\xi_x^{(\mu)}|e^{i\phi_x^{(\mu)}}$ and $\xi_y^{(\mu)}=|\xi_y^{(\mu)}|e^{i\phi_y^{(\mu)}}$ are the eigenvalues of the second derivative matrix of $G(\mathbf{k}_{\parallel})$ at the μ th extremal point.

The remaining integration over E will also be carried out using the variant of the saddle-point method for the case where there are no extremal points, i.e., the functions $Q^{(\mu)}(E)$ are monotonic. Note that, since $Q^{(\mu)}(E)$ is always a difference between a k point of positive velocity and a point of negative velocity, it is a typical case that this function is a monotonically increasing function of E . This is equivalent to the fact that the electron pockets of the surface $E_{\mathbf{k}}=E$ increase in size with E . Following the recipe of Ref. 46, we find that

$$\delta\Omega_{LR}=\frac{1}{D^2}\sum_{\mu}\text{Im}\{A^{(\mu)}e^{iQ^{(\mu)}D}\}, \quad \text{with}$$

$$A^{(\mu)}=-\frac{Sd^2}{2\pi^2}\frac{\exp\{-i(\phi_x^{(\mu)}+\phi_y^{(\mu)})/2\}T^{(\mu)}}{\sqrt{|\xi_x^{(\mu)}\xi_y^{(\mu)}|}[dQ^{(\mu)}(E)/dE]}, \quad (\text{A9})$$

where all the energy-dependent quantities including the derivative $[dQ^{(\mu)}(E)/dE]$ are evaluated at $E=E_f$. The above equation is the final and central result of this Appendix. Clearly, this formula is equivalent to that of Eq. (13) and the OEC has an oscillatory part coming from the real part of the quantity $Q^{(\mu)}$, i.e., the size of the Fermi-surface spanning vector, and a dumping factor resulting from the imaginary part of $Q^{(\mu)}$. In the light of an argument advanced in Refs. 17,18, in the limit of small disorder $\text{Im}\{Q^{(\mu)}\}=(1/\lambda_{\perp+}^{(\mu)})-(1/\lambda_{\perp-}^{(\mu)})$, where $\lambda_{\perp+}^{(\mu)}, \lambda_{\perp-}^{(\mu)}$ are the coherence lengths, closely related to the mean free paths of the quasiparticle states at the end points of the corresponding extremal vector. These mean free paths are given in the KKR-CPA method as the inverse of the half widths of the Lorentzian-like Bloch spectral functions (BSF's). The small disorder limit is proven to be correct in most of the random binary alloy cases, whose Fermi surfaces are well defined and the BSF well fitted to sums of Lorentzians.^{18,44,58} In this limit, the widths of the Lorentzian-like BSF's are small compared to the extremal vector size. Thus the corresponding mean free paths are much larger than the OEC periods.

We will close this Appendix by mentioning that we have considered a typical case for Fermi surface extremal vectors. Exceptions of course might exist and the results of this section should be modified. A simple example is the case where a spanning vector is extremal in one direction but constant in the perpendicular direction. In that case the treatment is different of course and the $1/D^2$ power law will be modified to a $1/D^{1.5}$ one.⁵⁹

*Author to whom correspondence should be addressed.

¹M.N. Baibich, J.M. Broto, A. Fert, F. Nguyen Van Dau, F. Petroff, P. Etienne, G. Creuzet, A. Friederich, and J. Chazelas, Phys. Rev. Lett. **61**, 2472 (1988).

²G. Binasch, P. Grunberg, F. Saurenbach, and W. Zinn, Phys. Rev. B **39**, 828 (1989).

³S.S.P. Parkin, N. More, and K.P. Roche, Phys. Rev. Lett. **64**, 2304 (1990).

⁴P. Bruno and C. Chappert, Phys. Rev. Lett. **67**, 1602 (1991).

⁵P. Bruno and C. Chappert, Phys. Rev. B **46**, 261 (1992).

⁶A. Cebollada, J.L. Martinez, J.M. Gallego, J.J. de Miguel, R.

Miranda, S. Ferrer, F. Batallan, G. Fillion, and J.P. Rebouillat, Phys. Rev. B **39**, 9726 (1989).

⁷*Ultrathin Magnetic Structures II*, edited by B. Heinrich and J.A.C. Bland (Springer-Verlag, Berlin, 1994).

⁸J.J. de Miguel, A. Cebollada, J.M. Gallego, R. Miranda, C.M. Schneider, P. Schuster, and J. Kirschner, J. Magn. Magn. Mater. **93**, 1 (1991).

⁹M.T. Johnson, S.T. Purcell, N.W.E. McGee, R. Coehoorn, J. aan de Stegge, and W. Hoving, Phys. Rev. Lett. **68**, 2688 (1992).

¹⁰Z.Q. Qiu, J. Pearson, and S.D. Bader, Phys. Rev. B **46**, 8659 (1992).

- ¹¹R. Allenspach and W. Weber, IBM J. Res. Dev. **42**, 7 (1998).
- ¹²P. Lang, L. Nordström, K. Wildberger, R. Zeller, and P.H. Dederichs, Phys. Rev. B **53**, 9092 (1996).
- ¹³L. Nordström, P. Lang, R. Zeller, and P.H. Dederichs, Phys. Rev. B **50**, 13 058 (1994).
- ¹⁴P.H. Dederichs, K. Wildberger, and R. Zeller, Physica B **237-238**, 239 (1997).
- ¹⁵J. Mathon, M. Villeret, R.B. Muniz, J.D.E. Castro, and D.M. Edwards, Phys. Rev. Lett. **74**, 3696 (1995).
- ¹⁶B. Lee and Y.-Ch. Chang, Phys. Rev. B **52**, 3499 (1995).
- ¹⁷N.N. Lathiotakis, B.L. Györfy, B. Újfalussy, and J. Staunton, J. Magn. Magn. Mater. **185**, 293 (1998).
- ¹⁸N.N. Lathiotakis, B.L. Györfy, and J.B. Staunton, J. Phys.: Condens. Matter **10**, 10 357 (1998).
- ¹⁹M.T. Johnson, R. Coehoorn, J.J. de Vries, N.W.E. McGee, J. aan de Stegge, and P.J.H. Bloemen, Phys. Rev. Lett. **69**, 969 (1992).
- ²⁰S.N. Okuno and K. Inomata, Phys. Rev. Lett. **70**, 1711 (1993).
- ²¹F. Herman, J. Sticht, and M. Van Schilfgaarde, J. Appl. Phys. **69**, 4783 (1991); in *Magnetic Thin Films, Multilayers, and Surfaces*, edited by S.S.P. Parkin, MRS Symposia Proceedings No. 231 (Materials Research Society, Pittsburgh, 1992), p. 195.
- ²²B. Gordon, W.M. Temmerman, B.L. Györfy, and G.M. Stocks, *Transition Metals—1977*, IOP Conference Proceedings No. 39 (Institute of Physics, London, 1978), p. 402.
- ²³W.J. O'Sullivan and J.E. Schirber, Phys. Rev. **181**, 1367 (1969).
- ²⁴S.S.P. Parkin, R. Bhadra, and K.P. Roche, Phys. Rev. Lett. **66**, 2152 (1991).
- ²⁵D. Pescia, D. Kerkmann, F. Schumann, and W. Gudat, Z. Phys. B: Condens. Matter **78**, 475 (1990).
- ²⁶W.F. Egelhoff, Jr. and M.T. Kief, Phys. Rev. B **45**, 7795 (1992).
- ²⁷J.P. Renard, P. Beauvillain, C. Dupas, K. Le Dang, P. Veillet, E. Vélú, C. Marlière, and D. Renard, J. Magn. Magn. Mater. **115**, L147 (1992).
- ²⁸D. Greig, M.J. Hall, C. Hammond, B.J. Hickey, H.P. Ho, M.A. Howson, M.J. Walker, N. Wisser, and D.G. Wright, J. Magn. Magn. Mater. **110**, L239 (1992).
- ²⁹J. Kohlhepp, S. Cordes, H.J. Elmers, and U. Gradmann, J. Magn. Magn. Mater. **111**, L231 (1992).
- ³⁰A. Kamijo and H. Igarashi, Jpn. J. Appl. Phys., Part 2 **31**, L1050 (1992).
- ³¹A. Schreyer, K. Bröhl, J.F. Anker, C.F. Majkrzak, Th. Zeidler, P. Bödeker, N. Metoki, and H. Zabel, Phys. Rev. B **47**, 15 334 (1993).
- ³²M.A. Howson, B.J. Hickey, J. Xu, D. Greig, and N. Wisser, Phys. Rev. B **48**, 1322 (1993).
- ³³D.M. Edwards, J. Mathon, R.B. Muniz, and M.S. Phan, Phys. Rev. Lett. **67**, 493 (1991); J. Phys.: Condens. Matter **3**, 4941 (1991).
- ³⁴M.D. Stiles, Phys. Rev. B **48**, 7238 (1993).
- ³⁵J. Kudrnovský, V. Drchal, R. Coehoorn, M. Sob, and P. Weinberger, Phys. Rev. Lett. **78**, 358 (1997).
- ³⁶P. Bruno, J. Kudrnovský, V. Drchal, and I. Turek, J. Magn. Magn. Mater. **165**, 128 (1997).
- ³⁷D.D. Koelling, Phys. Rev. B **59**, 6351 (1999).
- ³⁸N.N. Lathiotakis, B.L. Györfy, E. Bruno, B. Ginatempo, and S.S.P. Parkin, Phys. Rev. Lett. **83**, 215 (1999).
- ³⁹L. Szunyogh, B. Újfalussy, P. Weinberger, and J. Kollár, Phys. Rev. B **49**, 2721 (1994).
- ⁴⁰B. Újfalussy, N.N. Lathiotakis, B.L. Györfy, and J.B. Staunton, Philos. Mag. B **78**, 577 (1998).
- ⁴¹E. Bruno and B.L. Györfy, J. Phys.: Condens. Matter **5**, 2109 (1993).
- ⁴²E. Bruno, B.L. Györfy, and J.B. Staunton, in *Metallic Alloys: Experimental and Theoretical Perspectives*, Vol. 256 of NATO Advanced Study Institute, Series E: Applied Sciences, edited by J.S. Faulkner and R.G. Jordan (Kluwer Academic, Dordrecht, 1994), p. 321.
- ⁴³B. Velický, Phys. Rev. **184**, 614 (1969).
- ⁴⁴B.L. Györfy and G.M. Stocks, in *Electrons in Disordered Metals and at Metallic Surfaces*, Vol. 42 of NATO Advanced Study Institute, Series B: Physics, edited by P. Phariseau, B. Györfy, and L. Scheire (Plenum, New York, 1979).
- ⁴⁵I. Turek, V. Drchal, J. Kudrnovský, M. Sob, and P. Weinberger, *Electronic Structure of Disordered Alloys Surfaces and Interfaces* (Kluwer Academic, Dordrecht, 1996).
- ⁴⁶C. Bender and S. Orszag, *Advanced Mathematical Methods for Scientists and Engineers* (McGraw-Hill, New York, 1978), pp. 258–259.
- ⁴⁷M. Ablowitz and A. Fokas, *Complex Variables* (Cambridge University Press, Cambridge, 1997).
- ⁴⁸B. Heinrich, J.F. Cochran, M. Kowalewski, J. Kirschner, Z. Celinski, A.S. Arrot, and K. Myrtle, Phys. Rev. B **44**, 9348 (1991).
- ⁴⁹P. Bruno, Eur. Phys. J. B **11**, 83 (1999).
- ⁵⁰S.S.P. Parkin, R.F. Marks, R.F.C. Farrow, G.R. Harp, Q.H. Lam, and R.J. Savoy, Phys. Rev. B **46**, 9262 (1992).
- ⁵¹E. M. Lifshitz and L. P. Pitaevskii, *Statistical Physics, Part 2*, Landau and Lifshitz Course of Theoretical Physics (Pergamon, New York, 1980), Vol. 9, p. 259.
- ⁵²S. Berko, in *Electrons in Disordered Metals and at Metallic Surfaces* (Ref. 44), pp. 239–291.
- ⁵³*Magnetische Schichtsysteme, 30. Ferienkurs des Instituts für Festkörperforschung 1999*, edited by P.H. Dederichs, and P. Grünberg, (Forschungszentrum Jülich GmbH, Institut für Festkörperforschung, Jülich, 1999).
- ⁵⁴F.-J. Bobo, L. Hennen, M. Piecuch, and J. Hubsch, Europhys. Lett. **24**, 139 (1993); J. Phys.: Condens. Matter **6**, 2689 (1994).
- ⁵⁵S.S.P. Parkin, C. Chappert, and F. Herman, Europhys. Lett. **24**, 71 (1993).
- ⁵⁶D. Kalkstein and P. Soven, Surf. Sci. **26**, 85 (1971).
- ⁵⁷R. Coehoorn, Phys. Rev. B **44**, 9331 (1991).
- ⁵⁸E. Bruno, B. Ginatempo, E.S. Giuliano, A.V. Ruban, and Y. Vekilov, Phys. Rep. **249**, 353 (1994).
- ⁵⁹D.D. Koelling, Phys. Rev. B **50**, 273 (1994).